PROCEEDINGS OF SPIE

SPIEDigitalLibrary.org/conference-proceedings-of-spie

Polychromatic effects on incoherent imaging through anisoplanatic turbulence

Ryan J. Hall, Mark F. Spencer

Ryan J. Hall, Mark F. Spencer, "Polychromatic effects on incoherent imaging through anisoplanatic turbulence," Proc. SPIE 11135, Unconventional and Indirect Imaging, Image Reconstruction, and Wavefront Sensing 2019, 1113506 (6 September 2019); doi: 10.1117/12.2528502

SPIE.

Event: SPIE Optical Engineering + Applications, 2019, San Diego, California, United States

Polychromatic effects on incoherent imaging through anisoplanatic turbulence

Ryan J. Hall[a] and Mark F. Spencer[b]

[a]Georgia State University, 33 Gilmer St., Atlanta 30303, USA;
[b]Air Force Research Laboratory, Directed Energy Directorate, 3550 Aberdeen Ave SE, Kirtland AFB, Albuquerque, New Mexico 87117, USA

ABSTRACT

We present a numerical simulation of incoherent imaging of an extended object through distributed-volume atmospheric turbulence. As such, we can observe and quantify the effects of anisoplanitismin in the image plane of our optical system. Along with simulating the effects of anisoplantism, we aim to quantify the effects of polychromatic blurring in the image plane of our optical system. This outcome allows us to simulate the real-world scenario of a spectral filter with an effective bandpass. Using the spectral-slicing method, we define a square-response filter and discretely sample it at multiple wavelengths to simulate the polycromatic nature of our optical system. In turn, we find that the effects of polychromatic blurring are minimal, given modern-day narrowband filters. Thus, the use of monochromatic light is sufficient in simulating incoherent imaging; however, it is important to note that our results suggest that there may be a minor sampling error that would need to be addressed if the approach used here was to be expanded to an extremely broadband case.

Keywords: Atmospheric turbulence, atmospheric propagation, anisoplanatism, distribute-volumed turbulence, polychromatic, deep turbulence

1. INTRODUCTION

Incoherent optical waves propagating through the Earth's atmosphere encounter turbulent eddies, which manifest as randomly varying refractive indices. Given propagation from the object plane to the pupil plane, the waves will become distorted by these randomly varying refractive indices, and the resulting image plane will have considerable blurring. Using instruments known as wavefront sensors (WFSs), this blurring can be minimized via adaptive-optics and image-processing techniques. However, traditional WFSs will retrieve path-integrated phase information at a pupil plane of the total optical system. Using this information is typically valid under isoplanatic conditions (i.e., the blurring of the object is described by a linear, shift-invariant system with respect to irradiance). However, if an extended object is being imaged through distributed-volume atmospheric turbulence, then the blurring of the object is described by a linear, shift-varying system with respect to irradiance. The effects of this blurring is known as anisoplanatism. It is easy to see that if a WFS is able to obtain tomographic information, it will significantly improve our abilities to employ advanced adaptive-optics and image-processing techniques to deblur the resulting imagery. In order to accurately model these tomographic WFSs, it is important that they be tested with data that accurately simulates these anisoplanatic effects, along with other effects.[1]

With the above information in mind, in this paper we present the results from a new wave-optics model that demonstrates the imaging of incoherently illuminated extended objects through distributed-volume atmospheric turbulence along a homogeneous-propagation path. This model allows us generate data to test tomographic WFS designs with the effects of anisoplantism amongst others. For example, in this paper, we model the effects of polychromatic blurring, in addition to anisoplanatism. The common assumption found within the literature is that we can neglect the effects of polychromatic blurring. With that said, the reality is that the point spread function (PSF) (i.e., the irradiance of the impulse response) generated by an instance of turbulence is a function of wavelength. This outcome means that there are two main contributors to the varying PSFs in the image plane, wavelength and anisoplanatism. Therefore, in this paper we quantify the effects of polychromatic blurring (in addition to anisplanatism) using an image sharpness metric.

Send correspondence to R.J.H. at hall@astro.gsu.edu

Unconventional and Indirect Imaging, Image Reconstruction, and Wavefront Sensing 2019, edited by Jean J. Dolne, Mark F. Spencer, Markus E. Testorf, Proc. of SPIE Vol. 11135, 1113506
 · doi: 10.1117/12.2528502

In what follows, Section 2 discusses the setup of our simulation. Section 3 then provides an exploration for this simulation. Section 4 discusses the results found from our simulation, and Section 5 draws conclusions based on these results.

2. SIMULATION SETUP

This section includes all of the parameters used in our simulation. It also includes a description of our method for simulating incoherent imaging (via a superpostion integral) and how we simulate the effects of polychromatic blurring (via spectral slicing). In general, we simulate the effects of distributed-volume atmospheric turbulence using the split-step beam propagation method.[2] This method works by creating a number of discrete Kolmogorov phase screens along the propagation path. We ultimately propagate from the object plane to a phase screen via angular-spectrum propagation through vacuum. After, we repeat the process until we reach the pupil plane of our optical system (i.e., a collimated aperture). We then simulate propagation to the image plane by applying a thin-lens phase function and propagating to focus.

2.1 Parameters

A list of parameters are recorded in Table 1. All parameters are designed to satisfy Fresnel scaling (N_f), such that

$$N_f = \frac{L^2}{\lambda Z}, \tag{1}$$

where L is the square side length of the propagated field, λ is the wavelength, and Z is the propagation distance. The strength of turbulence is in the moderate-strong regime. This last statement is based on the amount of scintillation that would occur, given monochromatic light. The amount of scintillation can be quantified via the Rytov number (σ_χ^2). Another common metric to quantify the strength of turbulence is to compare the fried parameter (r_0) to the size of the pupil (D). This metric gives us a gauge for imaging resolution. The last metric we use to describe the distributed-volume atmospheric turbulence the isoplanatic angle (θ_0) relative to the diffraction angle (λ/D). This metric helps in quantifying the amount of anisoplantism present.

Table 1: Parameters used in the simulation. Throughout this paper, D is the circular-pupil diameter, r_0 is the Fried parameter, σ_χ^2 is the Rytov number, λ is central wavelength, and θ_0 is the isoplanatic angle

Pupil Diameter	0.4 m
Central Wavelength	632.8 nm
Grid Size	2048x2048 pixels
Side Length	1.2 m
Propagation Distance	1000 m
Target Length	7.91 cm
Target Width	1.58 cm
D/r_0	20
σ_χ^2	0.26
$\frac{\theta_0}{\lambda/D}$	3.26

2.2 Superposition integral

The proposed method to simulate incoherent imaging is based on the approach used by Bos and Roggemann.[3] Our method involves placing a point source at every pixel where the object exists and propagating each one independently via the split-step beam propagation method. The point sources are generated by creating a unit amplitude square aperture that is twice the size of the true aperture in the pupil plane. We then back propagate through vacuum to the object plane. By adding a specific amount of tilt phase, prior to back propagation, we can control where the sinc-like point sources will be centered in the object plane. This tilt is how we place each point source at every pixel where the object exists. Then the point sources are propagated through the distributed-volume atmospheric turbulence (again, using the split-step beam propagation method) to the pupil plane where a thin lens is used to collimate and aperture. Now, each point source is ready to be propagated to the image plane.

In the image plane, we can sum up the contributions of each point source via a superposition integral with respect to irradiance, such that

$$g_{Ii}(x,y) = \int\int_{\infty}^{\infty} g_{Io}(\xi,\eta)h^2(x,y;\xi,\eta)d\xi d\eta. \quad (2)$$

Here, each point-source irradiance pattern is known as a PSF (h^2), where at a given position (ξ,η), g_{Io} is the irradiance of the object in the object plane, and g_{Ii} is the irradiance of the object in the image plane. The difference between our method and Bos and Roggemann[3] or Hardie et al.[4] is the number of point sources used along the object. Both research efforts place a point source at every isoplanatic angle along the object and interpolate over the "block PSFs" to obtain the missing PSFs. In comparison, our method could be viewed as a more rigorous method; however, a direct comparison needs to be performed to quantify this claim.

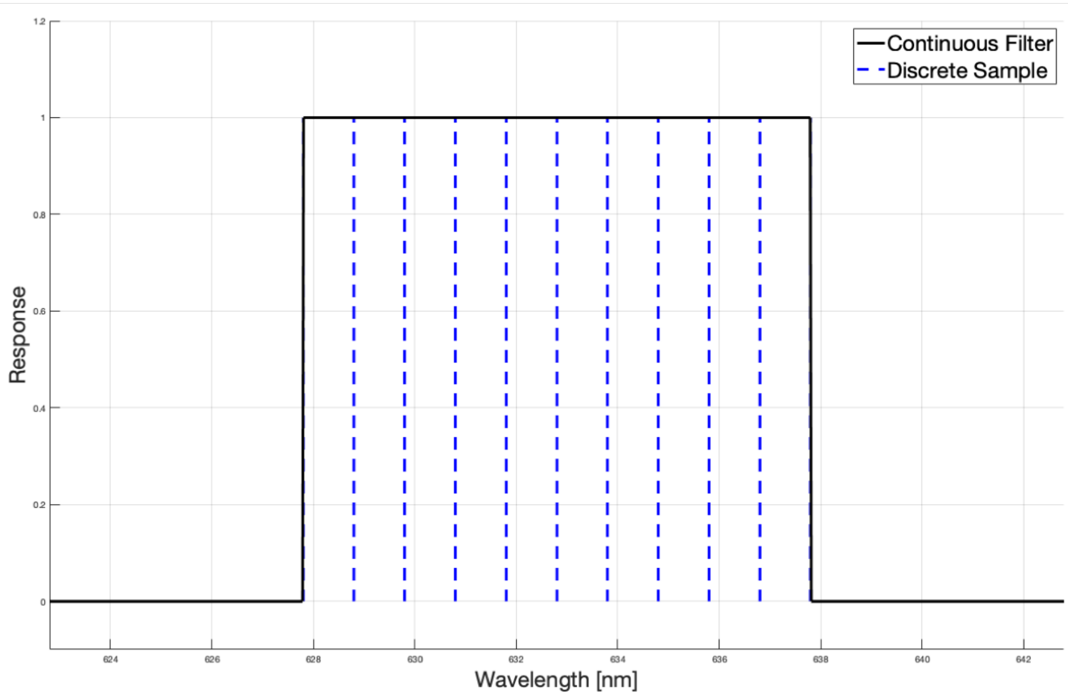

Figure 1: Example of the Spectral Slicing method on a square response filter centered at a wavelength of 632.8nm. This example includes a total width of 10nm with 1nm sampling.

2.3 Spectral Slicing

The incoherent propagation process has to repeated for every wavelength that needs to be tested. Put another way, if we simulate a 10nm filter sampled every 1nm, we must propagate each point source on the object 11 times (once for each wavelength sampled in the filter). This method of discretely sampling a spectrum is known as the spectral-slicing method.[5,6] In turn,this method allows for independent propagation of each wavelength, such that each wavelength interacts with the distributed-volume aberrations appropriately. A visual example of this method is available in Fig. 1.

3. SIMULATION EXPLORATION

In this paper, we wanted to explore the effects of anisoplanatism, as well as polychromatic blurring in the image plane of our optical system. To accomplish this goal, we created a three-bar object (physical characteristics found in Table 1) and assumed that it was passively illuminated via a spectrally gray source. As stated in Section 2.2, we simulated incoherent imaging of this three-bar object through distributed-volume atmospheric turbulence by propagating independent point sources, with a specified wavelength, via the split-step beam propagation method from every pixel where our three-bar target exists (see Fig. 2).

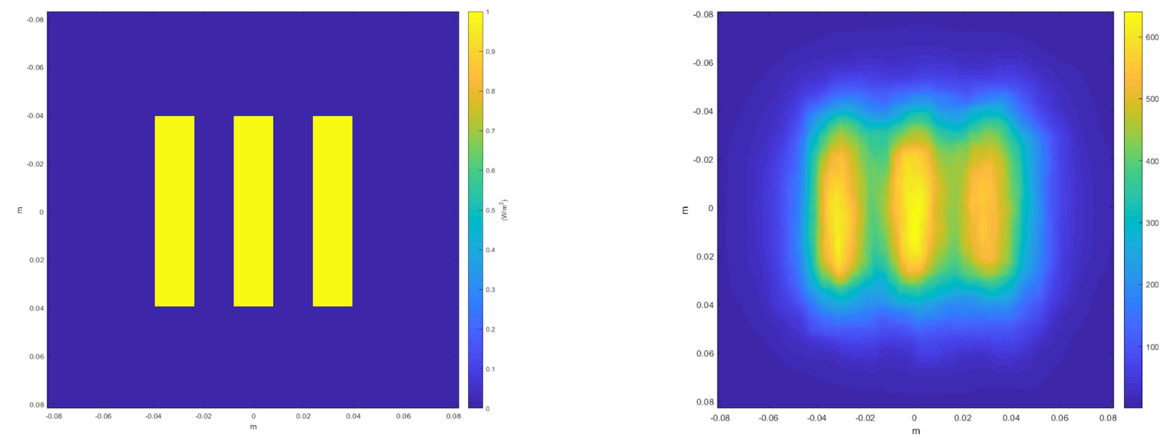

(a) (b)

Figure 2: The effects of anisoplanatism. (a) shows the three bar target amplitude in the object plane (no propagation). (b) shows the three bar target amplitude in the image plane after propagation through distributed-volume atmospheric turbulence. The results presented here are for the central wavelength given in Table 1.

By repeating the procedure used to create Fig. 2 for a range of wavelengths, as described in Section 2.3, we can also account for the effects of polychromatic blurring. We do so in the next section.

4. RESULTS AND DISCUSSION

The quality of the imaged object was obtained using a sharpness metric adapted from that of Thurman and Fienup.[7] In their work, they defined a sharpness metric in order to estimate the phase errors from image-sharpening algorithms. We define a similar metric that describes the sharpness of the received irradiance in the image plane of our simulations. The sharpness (S) is defined as a function of the received irradiance field (I), such that

$$S = \frac{\Sigma(I^2)}{(\Sigma I)^2}. \quad (3)$$

We then ran our simulations for a number of filter widths ranging from 0nm (monochromatic) to 10nm with 1nm spectral sampling. In addition, we ran another set of filters ranging for 0 to 50nm with 5nm sampling. The sampling size and filter widths were chosen do to time constraints and computational resources. The results of these scenarios can be found in Fig. 3. Since the sharpness metric seems to drop slowly (seen in the range of the vertical axis in Fig. 3), we also checked the validity of the simulations by examining the cross section of the irradiance in the image plane for two distinct wavelengths. This result can be found in Fig. 4.

Figure 4 suggests that our results are producing realistic features. This is said because Fig. 4 shows more power being spread out between the bars for bluer wavelengths than redder wavelengths. It is generally expected that bluer wavelengths will experience more blurring due to distributed-volume atmospheric turbulence, as

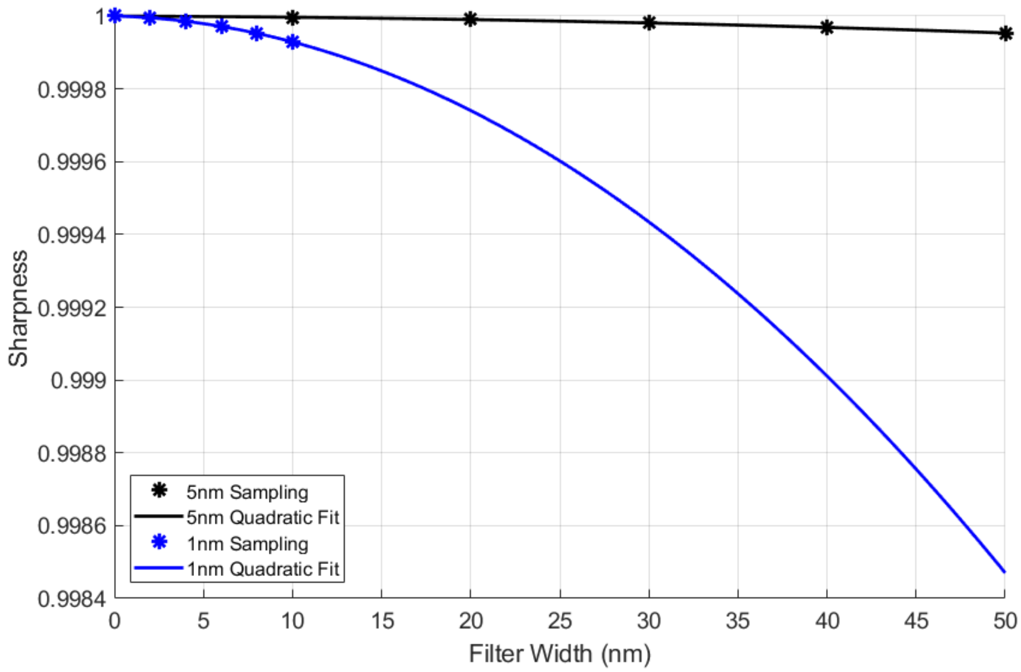

Figure 3: Image sharpness (normalized to monochromatic filter) vs. filter width. Plotted are the results from two test cases: black (5nm sampling) and blue (1nm sampling). Notice that both trials test five different filters and have been fitted with quadratics to show trends. The 1nm sampling curve shows a more steep curve which is noticeable when expanded out to 50nm filter width. It is important to notice the range of the vertical axis, seeing that it only decreases at the third decimal place at the widest filter width.

seen in the image plane. According to the plot found in Fig. 3, we can also assume that given modern-day filters (widths on the order of 10s of nanometers) it is appropriate to simulate incoherent imaging with monochromatic light. However, it is important to note that this outcome only holds true for narrowband light. For broadband light, the sampling issue becomes more apparent in the results. This may suggest that when simulating extremely broadband light (100s of nanometers), the spectral-slicing method presented here is most likely necessary. Moreover, our results also suggest that further exploration is needed to determine the necessary number of spectral slices.

5. CONCLUSIONS

In this paper, We presented a new way to simulate incoherent imaging through distributed-volume atmospheric turbulence. In turn, we observed and quantified the effects of anisoplanitism and polychromatic blurring in the image plane of our optical system. This outcome allowed us to simulate the real-world scenario of a spectral filter with an effective bandpass. Using the spectral-slicing method, we defined a square-response filter and discretely sampled it at multiple wavelengths to simulate the polycromatic nature of our optical system. In turn, we found that the effects of polychromatic blurring are minimal, given modern-day narrowband filters. Thus, the use of monochromatic light is sufficient in simulating incoherent imaging. Future efforts should note that our results suggest that there may be a minor sampling error that would need to be addressed if the approach used here was to be expanded to an extremely broadband case.

REFERENCES

[1] S. M. Jefferies, M. Lloyd-Hart, E. K. Hege, and J. Georges, "Sensing wave-front amplitude and phase with phase diversity," Appl. Opt. 41, 2095-2102 (2002).

Figure 4: Cross section of irradiance in the image plane of the optical system. The figure cuts through a horizontal section of the output so that all three bars can be clearly seen. This is done for two separate wavelengths (50nm apart) to show that the simulation is behaving as expected. It can be clearly seen that in between the bars there is more irradiance in the bluer wavelength.

[2] J. D. Schmidt, *Numerical Simulation of Optical Wave Propagation using MATLAB*, SPIE Press, Bellingham, Washington (2010).

[3] J. P. Bos, M. C. Roggeman, "Technique for simulating anisoplanatic image formation over long horizontal paths," Opt. Eng. 51 (2012).

[4] R. C. Hardie et al., "Simulation of anisoplanatic imaging through optical turbulence using numerical wave propagation with new validation analysis," Opt. Eng. 56 (2017).

[5] N. R. Van Zandt, J. E. McCrae, M. F. Spencer, M. J. Steinbock, M. W. Hyde, and S. T. Fiorino, "Polychromatic wave-optics models for image-plane speckle. 1. Well-resolved objects," App. Opt. 57, 4090-4102 (2018).

[6] N. R. Van Zandt, M. F. Spencer, M. J. Steinbock, B. M. Anderson, M. W. Hyde, and S. T. Fiorino, "Polychromatic wave-optics models for image-plane speckle. 2. Unresolved objects," App. Opt. 57, 4103-4110 (2018).

[7] S. T. Thurman and J. R. Fienup,"Phase-error correction in digital holography," J. Opt. Soc. Am. A 25, 983-994 (2001).